The American Journal of Pathology, Vol. 184, No. 7, July 2014

The American Journal of
PATHOLOGY
ajp.amjpathol.org

CELL INJURY, REPAIR, AGING, AND APOPTOSIS

MFG-E8 Regulates Angiogenesis in Cutaneous Wound Healing

Akihiko Uchiyama,* Kazuya Yamada,* Sachiko Ogino,* Yoko Yokoyama,* Yuko Takeuchi,* Mark C. Udey,† Osamu Ishikawa,* and Sei-ichiro Motegi*

From the Department of Dermatology, Gunma University Graduate School of Medicine, Maebashi, Japan; and the Dermatology Branch,† Center for Cancer Research, National Cancer Institute, NIH, Bethesda, Maryland*

Accepted for publication March 21, 2014.

Address correspondence to Sei-ichiro Motegi, M.D., Ph.D., Department of Dermatology, Gunma University Graduate School of Medicine, 3-39-22 Showa, Maebashi, Gunma 371-8511, Japan. E-mail: smotegi@gunma-u.ac.jp.

Our research group recently demonstrated that pericytes are major sources of the secreted glycoprotein and integrin ligand lactadherin (MFG-E8) in B16 melanoma tumors, and that MFG-E8 promotes angiogenesis via enhanced PDGF–PDGFRβ signaling mediated by integrin–growth factor receptor crosstalk. However, sources of MFG-E8 and its possible roles in skin physiology are not well characterized. The objective of this study was to characterize the involvement of MFG-E8 in skin wound healing. In the dermis of normal murine and human skin, accumulations of MFG-E8 were found around $CD31^+$ blood vessels, and MFG-E8 colocalized with $PDGFR\beta^+$, αSMA^+, and $NG2^+$ pericytes. MFG-E8 protein and mRNA levels were elevated in the dermis during full-thickness wound healing in mice. MFG-E8 was diffusely present in granulation tissue and was localized around blood vessels. Wound healing was delayed in MFG-E8 knockout mice, compared with the wild type, and myofibroblast and vessel numbers in wound areas were significantly reduced in knockout mice. Inhibition of MFG-E8 production with siRNA attenuated the formation of capillary-like structures *in vitro*. Expression of MFG-E8 in fibrous human granulation tissue with scant blood vessels was less than that in granulation tissue with many blood vessels. These findings suggest that MFG-E8 promotes cutaneous wound healing by enhancing angiogenesis. *(Am J Pathol 2014, 184: 1981–1990; http://dx.doi.org/10.1016/j.ajpath.2014.03.017)*

Wound healing is a dynamic process involving angiogenesis, production of soluble mediators and extracellular matrix, and migration of various types of cells, including keratinocytes, fibroblasts, macrophages, and leukocytes. Dysregulation of this interactive process may result in delayed wound healing, as is seen in chronic skin ulcers or scarring. Wound healing has three temporally overlapping phases: inflammation, tissue formation, and remodeling.[1,2] The inflammation phase occurs immediately after wounding. It is characterized by hypoxia with fibrin clot formation, as well as recruitment of neutrophils and platelets. Tissue formation occurs 2 to 10 days later and is characterized by epithelialization, formation of granulation tissue and new blood vessels, and accumulation of macrophages and fibroblasts. Activated macrophages release growth factors, such as vascular endothelial growth factor (VEGF) and platelet-derived growth factor (PDGF), and initiate angiogenesis. PDGF receptor β (PDGFRβ) signaling is essential for angiogenesis and for recruitment, proliferation, and normal function of fibroblasts and pericytes during the tissue-formation phase.[3] Blockade of VEGF receptor signaling and PDGFRβ signaling inhibits angiogenesis and results in delayed wound healing,[3,4] indicating that angiogenesis is critical for normal wound healing.

The secreted glycoprotein lactadherin was initially identified as a component of milk fat globules and is here referred to as milk fat globule-EGF factor 8 (MFG-E8); other names in the literature include secreted protein containing epidermal growth factor (EGF) repeats and discoidin/F5/8 domains 1, or SED1. MFG-E8 comprises two N-terminal EGF-like domains, and two C-terminal discoidin-like domains (C1 and C2) share homology with blood coagulation factors V and VIII.[5–9] One EGF-like domain (E2) contains an RGD

Supported in part by a grant from Adaptable and Seamless Technology Transfer Program of the Japan Science and Technology Agency, a grant from the Uehara Memorial Foundation (S.M.), and the Intramural Program of the NIH, Center for Cancer Research, National Cancer Institute (M.C.U.).

A.U. and S.M. contributed equally to this work.

Disclosures: None declared.

http://dx.doi.org/10.1016/j.ajpath.2014.03.017

consensus integrin-binding motif, and MFG-E8 binds to integrin αvβ3/5.[7−11] The C-terminal domains of MFG-E8 can bind to negatively charged and oxidized phospholipids,[12,13] facilitating opsonization of apoptotic cells for uptake by phagocytes.[10,14] This process has been reported to contribute to autoimmunity, mastitis, sepsis, atherosclerosis, and Alzheimer disease.[15−19] Interactions of MFG-E8 with CD51 (integrin αv) have also been implicated in regulation of angiogenesis and mammary gland branching,[11,20] and interactions mediated via the C1 domain are thought to be important for sperm−egg binding and collagen turnover.[21,22]

Our research group has previously demonstrated that MFG-E8 enhances angiogenesis in tumors and in oxygen-induced retinopathy in mice.[23] We determined that pericytes and/or pericyte precursors are important sources of MFG-E8 *in vivo*, that MFG-E8 enhances angiogenesis via actions on pericytes as well as endothelial cells (ECs), and that MFG-E8 can be effectively targeted with therapeutic benefit.[23] In murine melanomas and in retinas of mice with oxygen-induced retinopathy, MFG-E8 colocalized with pericytes rather than with ECs, and pericytes purified from tumors contained large amounts of MFG-E8 mRNA. Tumor- and retinopathy-associated angiogenesis was diminished in MFG-E8 knockout (KO) mice, and pericyte coverage of neovessels was also reduced. Inhibition of MFG-E8 production by pericyte/pericyte precursor-like 10T1/2 cells using siRNAs, or inhibition of MFG-E8 action with some anti−MFG-E8 antibodies, attenuated PDGF-BB−induced 10T1/2 cell migration, but did not affect proliferation or differentiation.[23] We have also determined that MFG-E8 produced by 10T1/2 cells associated with integrin αv and PDGFRβ on cell surfaces after PDGF-BB treatment, altered the distribution of PDGFRβ within cells and delayed PDGF-BB−stimulated degradation of PDGFRβ, thereby enhancing PDGFRβ signaling mediated by integrin−growth factor receptor crosstalk.[24]

In a study of MFG-E8, epithelial tissues, and wound healing, Bu et al[25] found that MFG-E8 promotes the migration of intestinal epithelial cells via a PKCε-dependent mechanism engaged by binding of MFG-E8 to phosphatidylserine. Their findings indicate that MFG-E8 is involved in the maintenance of intestinal epithelial homeostasis and the promotion of mucosal healing. The possible role of MFG-E8 in cutaneous wound healing has not been studied previously. In the present study, we analyzed skin wound healing using MFG-E8 wild-type (WT) and KO mice. We demonstrate that MFG-E8 production was increased and that MFG-E8 accumulated in granulation tissue during wound healing, and that wound healing in MFG-E8 KO mice was delayed. We relate delayed wound healing to diminished angiogenesis and myofibroblast infiltration in wounds in MFG-E8 KO mice.

Materials and Methods

Mice

MFG-E8 KO mice were generated, characterized, and genotyped as described previously.[23,26] Heterozygous founders were speed-backcrossed to C57BL/6 or BALB/c mice to generate animals with appropriate and uniform genetic backgrounds using the Speed Congenics Services of the Laboratory Animal Sciences Program at the National Cancer Institute−Frederick Center for Cancer Research (NIH, Bethesda, MD). MFG-E8−deficient mice were generated by interbreeding homozygous animals carrying the targeted MFG-E8 allele. Control animals were purchased from Japan SLC (Hamamatsu, Japan). Eight- to twelve-week-old C57BL/6 or BALB/c mice were used for all experiments. Mice were bred and maintained at the Institute of Experimental Animal Research of Gunma University Graduate School of Medicine under specific pathogen−free conditions. Mice were handled in accordance with the animal care guidelines of Gunma University.

Human Skin and Granulation Tissues

Normal human skin was obtained from the forearm of healthy volunteers. For the examination of human granulation tissue, normal and fibrous granulation tissue specimens were obtained from patients with decubitus ulcers. Ethics approval was granted by the local research ethics committee. All patients and volunteers provided written informed consent before participation. This study was conducted according to the Declaration of Helsinki principles.

Antibodies

The following antibodies were used: rat anti-mouse CD31 monoclonal antibody (mAb) (MEC13.3; BD Biosciences, San Jose, CA), rabbit anti-mouse NG2 polyclonal antibody (pAb) (EMD Millipore, Billerica, MA), rat anti-mouse PDGFRβ mAb (eBioscience, San Diego, CA), rat anti-mouse CD68 mAb (Bio-Rad Laboratories, Hercules, CA), mouse anti−α-smooth muscle actin (SMA) mAb (Sigma-Aldrich, St. Louis, MO), rabbit anti-human CD31 pAb (Abcam, Cambridge, UK), rabbit anti-human αSMA pAb (Abcam), and mouse anti-human MFG-E8 pAb (R&D Systems, Minneapolis, MN). Secondary antibodies conjugated with Alexa Fluor 488 or Alexa Fluor 568 were obtained from Life Technologies (Carlsbad, CA). Rabbit anti-mouse MFG-E8 pAb was generated and characterized in our laboratory as described previously.[23,24]

Immunofluorescence Staining

For whole-mount staining of ear skin, mouse ears were excised and split into dorsal and ventral halves, and cartilage and fat were removed. Skin sheets (including both dermis and epidermis) were fixed in cold acetone−methanol−water (2:2:1) for 10 minutes or in 4% paraformaldehyde for 30 minutes. After blocking with 3% nonfat dry milk−PBS supplemented with 5% normal goat serum for 1 hour at room temperature, sections were stained with the antibody of interest, followed by the secondary antibody conjugated with Alexa Fluor 488 or Alexa Fluor 568. Immunofluorescence staining of frozen sections and analysis was performed as

described previously.[23,24] Frozen sections (4 μm thick) prepared from murine and human skin were fixed in 4% paraformaldehyde in PBS for 30 minutes. After blocking with 3% nonfat dry milk−PBS supplemented with either 5% normal donkey serum or 5% normal goat serum for 1 hour at room temperature, sections were stained with the antibody of interest followed by the secondary antibody conjugated with Alexa Fluor 488 or Alexa Fluor 568. Sections were counterstained with to visualize nuclei and were mounted in ProLong Gold antifade reagent (Life Technologies).

Wound Healing Model and Analysis

Full-thickness wounds were made and examined as described previously.[27,28] In brief, mice were anesthetized, shaved, and cleaned with 70% ethanol. Two 5-mm full-thickness excisional dorsal skin wounds were made on each side of the midline with a sterile disposable biopsy punch (Kai Industries, Gifu, Japan). Wounds were covered by film dressings (Permeroll; Nitto Denko, Osaka, Japan). Wound sites were digitally photographed at various time points after wounding, and wound areas were measured on the images using ImageJ software version 1.46r (NIH, Bethesda, MD). Changes in wound area are expressed as percentage of initial wound area.

To assess effects of recombinant MFG-E8 (rMFG-E8) on wound healing in KO mice, 400 ng rMFG-E8 (R&D Systems, Minneapolis, MN) per 30 μL PBS or the same concentrations of bovine serum albumin was injected into the dermis around the wound every day after wounding until the closure of wound.

RT-qPCR

Total RNA was isolated using RNeasy mini kits (Qiagen, Valencia, CA) and was subjected to reverse transcription with use of a SuperScript III first-strand synthesis system (Life Technologies) according to the manufacturer's instructions. Real-time quantitative reverse transcription PCR (RT-qPCR) was performed using a TaqMan system (Life Technologies) with ABI 7300 real-time PCR instrumentation (Life Technologies) according to the manufacturer's instructions. TaqMan probes and primers for MFG-E8, CD31, αSMA, CD68, and GAPDH were purchased from Life Technologies. As an internal control, levels of GAPDH were quantified in parallel with target genes. Normalization and fold changes were calculated using the comparative C_T method.

MFG-E8 Knockdown Experiments and Capillary-Like Structure Formation Assay

Mouse C3H/10T1/2 cells were kindly provided by Dr. T. Iso (Department of Medicine and Biological Science, Gunma University, Maebashi, Japan). Human umbilical vein endothelial cells (HUVECs) were purchased from ATCC (Manassas, VA). 10T1/2 cells were maintained in BME medium (Life Technologies) supplemented with 10% heat-inactivated fetal bovine serum, 2 mmol/L L-glutamine, 100 U/mL penicillin, 100 μg/mL streptomycin and were used before passage 10. HUVECs were maintained in EBM-2 basal medium (Lonza, Basel, Switzerland; Walkersville, MD) supplemented with EGM-2 SingleQuots kit with growth

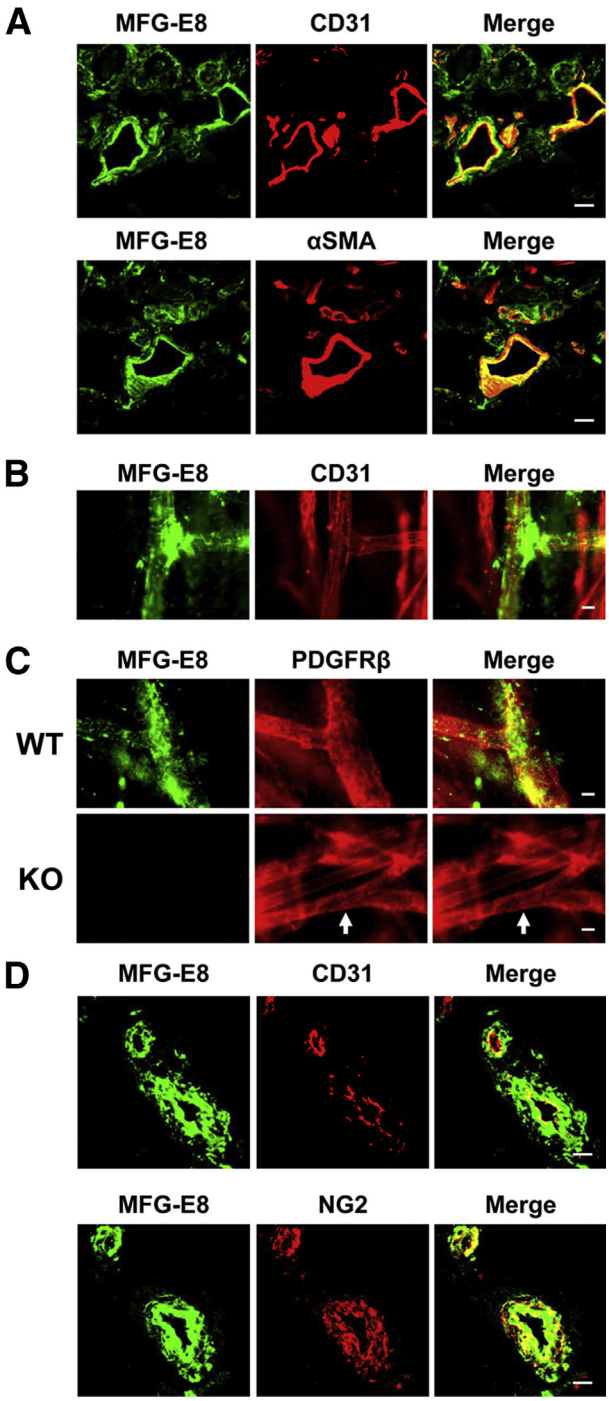

Figure 1 MFG-E8 localizes in close proximity to pericytes/vascular smooth muscle cells in the dermis of mouse and human skin. **A:** Localization of MFG-E8 in relationship to ECs ($CD31^+$) or pericytes (αSMA^+) in C57BL/6 mouse dermis. **B:** Localization of MFG-E8 in relationship to ECs ($CD31^+$) in the dermis of whole mount of C57BL/6 mouse ear skin. **C:** Localization of MFG-E8 in relationship to pericytes ($PDGFR\beta^+$) (**arrows**) in the dermis of whole mount of ear skin from MFG-E8 WT and KO C57BL/6 mice. **D:** Localization of MFG-E8 in relationship to ECs ($CD31^+$) and pericytes ($NG2^+$) in human dermis in frozen skin sections. Scale bar = 20 μm.

factors, cytokines, and supplements (Lonza). siRNAs specific for mouse and human MFG-E8 mRNA were designed with Qiagen. The targeting sequences were as follows: mouse MFG-E8 siRNA, 5′-AAGCGGTGGAGACAAGGAGTT-3′); human MFG-E8 siRNA, 5′-TACAGCCTTAATGGACACGAA-3′. siRNAs and AllStars negative control siRNA were purchased from Qiagen. To inhibit MFG-E8 production, 5×10^5 10T1/2 cells and HUVECs per 60-mm plate were transfected with 10 nmol/L siRNA using HiPerFect transfection reagent (Qiagen).

The capillary-like structure formation assay was performed as described previously.[29,30] At 24 hours after siRNA transfection, 2.5×10^4 HUVECs and/or 2.5×10^4 10T1/2 cells were cultured in solidified Matrigel (200 μL/well in 24-well plates) (BD Biosciences) and were incubated at 37°C. After 3 hours, six random fields were chosen in each well, and the total length of capillary-like structures was quantified using ImageJ software. To examine the effects of MFG-E8 siRNA, MFG-E8 mRNA levels were assessed by RT-qPCR immediately after the tube formation assay. Human and mouse MFG-E8 protein secreted into the medium during a 24-hour incubation were assessed with the use of ELISA kits (R&D Systems).

Statistical Analysis

P values were calculated using Student's *t*-test (two-sided) or by analysis of one-way analysis of variance followed by Bonferroni's post hoc test. Data are expressed as means ± SEM, and numbers of experiments (*n*) are indicated.

Results

Localization of MFG-E8 in Close Proximity to Pericytes/Vascular Smooth Muscle Cells in Dermis of Murine and Human Skin

To localize MFG-E8 in normal murine skin, immunofluorescence staining of vertical sections of back skin and whole mounts (epidermis and dermis) of normal C57BL/6 mouse ear skin was performed. Accumulations of MFG-E8 were found around $CD31^+$ ECs in the dermis (Figure 1, A and B, and Supplemental Figure S1). MFG-E8 deposits frequently occurred in proximity to vascular branch points (Figure 1B). MFG-E8 also colocalized with α-smooth muscle actin-positive (αSMA^+) or $PDGFR\beta^+$ pericytes in the dermis (Figure 1, A and C and Supplemental Figure S1). MFG-E8 staining was not observed in skin from MFG-E8 KO mice, confirming the specificity of our antibody (Figure 1C). These

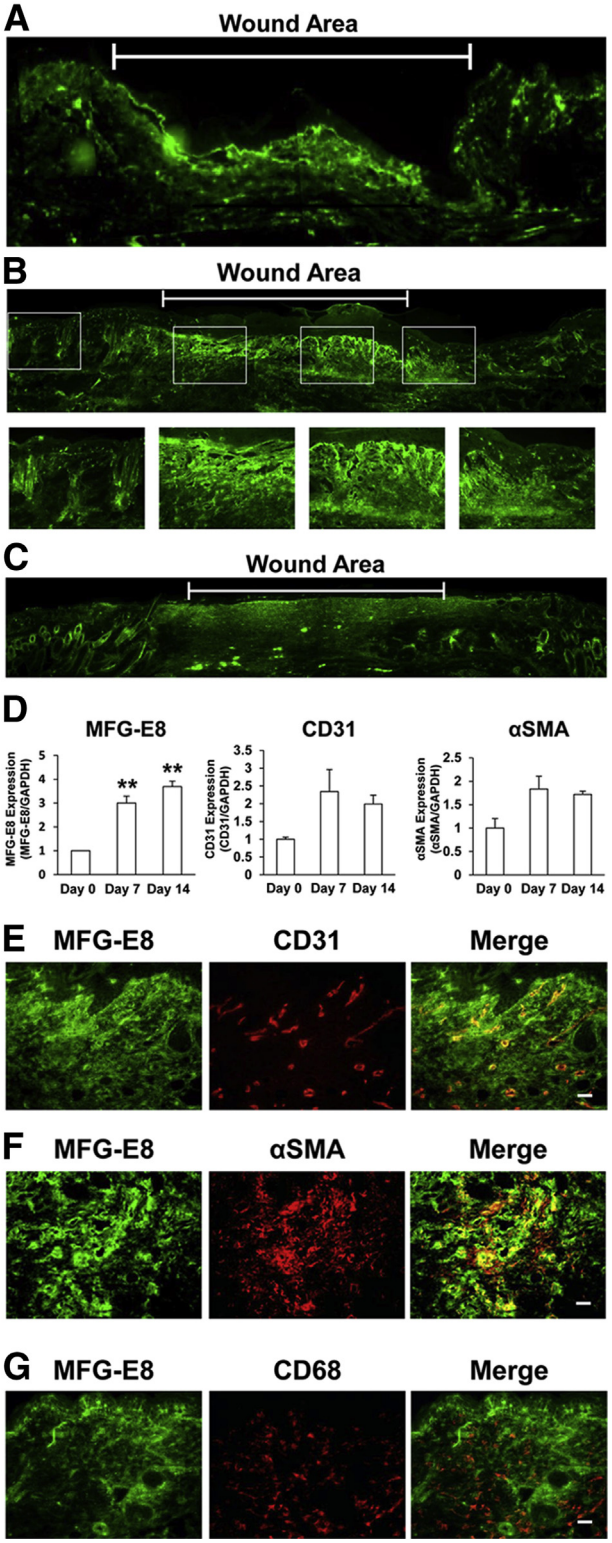

Figure 2 MFG-E8 expression is enhanced in the dermis and granulation tissue and around blood vessels during wound healing in mice. **A–C:** Localization and expression of MFG-E8 during skin wound healing in C57BL/6 mice as revealed by immunofluorescence staining at days 4 (**A**), 7 (**B**), and 14 (**C**) after wounding. **Boxed areas** in **B** are shown enlarged in the corresponding individual images. **D:** RT-qPCR quantification of MFG-E8, CD31, and αSMA mRNA levels in wound areas at 0, 7, and 14 days after wounding, expressed relative to mRNA levels at day 0. **E–G:** Localization of MFG-E8 in relationship to ECs ($CD31^+$) (**E**), pericytes/myofibroblasts (αSMA^+) (**F**), and macrophages ($CD68^+$) (**G**) in granulation tissue at 7 days after wounding. Data are expressed as means ± SEM, determined in three independent experiments. $^{**}P < 0.01$, analysis of variance followed by Bonferroni's post hoc test. Scale bar = 20 μm.

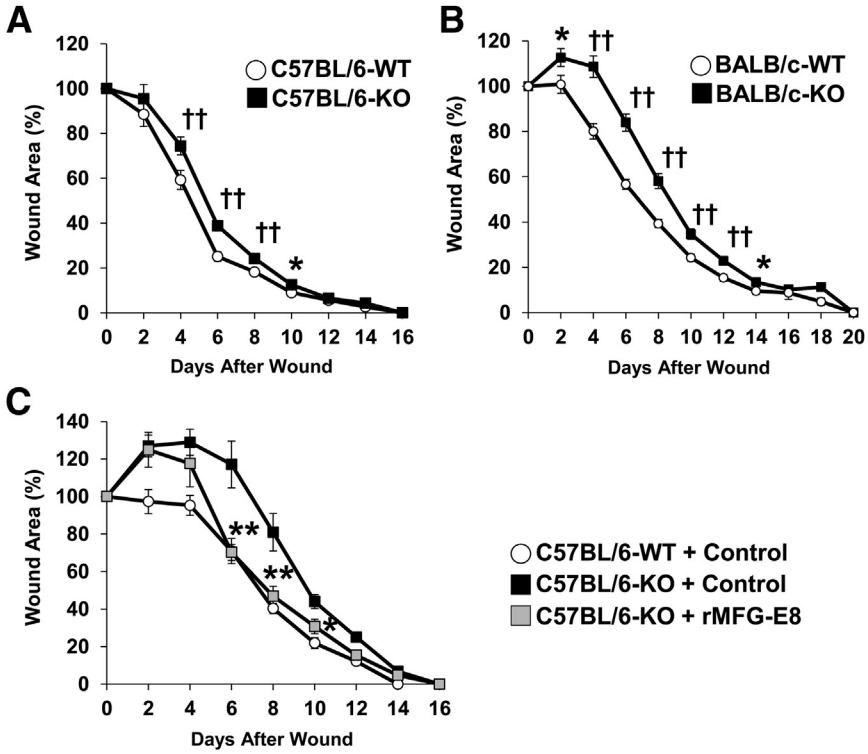

Figure 3 Skin wound healing is delayed in MFG-E8 KO mice. **A** and **B:** Percent wound area at each time point relative to the original wound area in MFG-E8 WT and KO C57BL/6 mice (**A**) and BALB/c mice (**B**). **C:** Percent wound areas at each time point relative to the original wound area in MFG-E8 WT C57BL/6 mice treated with control bovine serum albumin and in KO C57BL/6 mice treated with control bovine serum albumin or rMFG-E8. Data are expressed as means ± SEM. $*P < 0.05$, $**P < 0.01$, analysis of variance followed by Bonferroni's post hoc test; $^{\dagger\dagger}P < 0.01$, Student's *t*-test. $n = 6$ (**C**); $n = 24$ (**A**, KO); $n = 30$ (**A**, WT); $n = 34$ (**B**) for each time point and group.

results are consistent with our previous studies identifying pericytes as important sources of MFG-E8 in melanoma tumors *in vivo*.[23] We also analyzed the distribution of MFG-E8 in normal human skin. Staining of human skin sections revealed that MFG-E8 staining occurred almost exclusively in close proximity to $CD31^+$ blood vessels (Figure 1D), and MFG-E8 colocalized with $NG2^+$ pericytes (Figure 1D). These results suggest that MFG-E8 localizes in close proximity to pericytes/vascular smooth muscle cells in the dermis of murine and human skin.

Enhancement of MFG-E8 Expression in the Dermis and Granulation Tissue with Localization Near Blood Vessels during Wound Healing

We next examined the expression and localization of MFG-E8 during wound healing in murine skin. At 4 days after wounding, MFG-E8 staining was increased in granulation tissue in wound areas, compared with that in surrounding areas (Figure 2A). Furthermore, at 7 days after wounding, MFG-E8 staining was significantly increased in wound areas and was distributed diffusely in granulation tissue (Figure 2B). At 14 days after wounding, MFG-E8 expression persisted in the dermis of wound areas (Figure 2C). Expression of MFG-E8 mRNA in wound areas was examined by RT-qPCR. MFG-E8 mRNA levels at 7 and 14 days after wounding were three- to fourfold greater than at baseline (Figure 2D). CD31 and αSMA mRNA expression was also increased at 7 and 14 days after wounding (Figure 2D). These results suggest that protein and mRNA levels of MFG-E8 in granulation tissue were enhanced during wound healing, and that expression of EC and pericyte markers was also increased.

Next, we examined the precise distribution of MFG-E8 in granulation tissue in relation to ECs, pericytes, and macrophages. At 7 days after wounding, MFG-E8 was present diffusely in granulation tissue, with enhanced accumulation around $CD31^+$ ECs (Figure 2E). MFG-E8 staining overlapped more extensively with αSMA, suggesting that αSMA^+ pericytes or myofibroblasts in granulation tissue may be an important source of MFG-E8 (Figure 2F). Notably, MFG-E8 did not colocalize with $CD68^+$ macrophages (Figure 2G). These results indicate that MFG-E8 increases in granulation tissue and suggest that it might regulate angiogenesis in wound healing.

Delayed Cutaneous Wound Healing in MFG-E8 KO Mice

To assess the role of MFG-E8 in wound healing *in vivo*, we compared the kinetics of cutaneous wound healing in MFG-E8 WT and KO mice on C57BL/6 and BALB/c genetic backgrounds. In C57BL/6 mice, wound healing was significantly delayed (by approximately 1 day) in MFG-E8 KO mice from 4 to 10 days after wounding, compared with WT mice (Figure 3A). In BALB/c mice, wound healing was significantly delayed (by approximately 2 days) in MFG-E8 KO mice from 2 to 14 days after wounding, compared with WT mice (Figure 3B). Furthermore, rMFG-E8 treatment negated the delay in wound healing in MFG-E8 KO mice (Figure 3C). These findings suggest that MFG-E8 positively

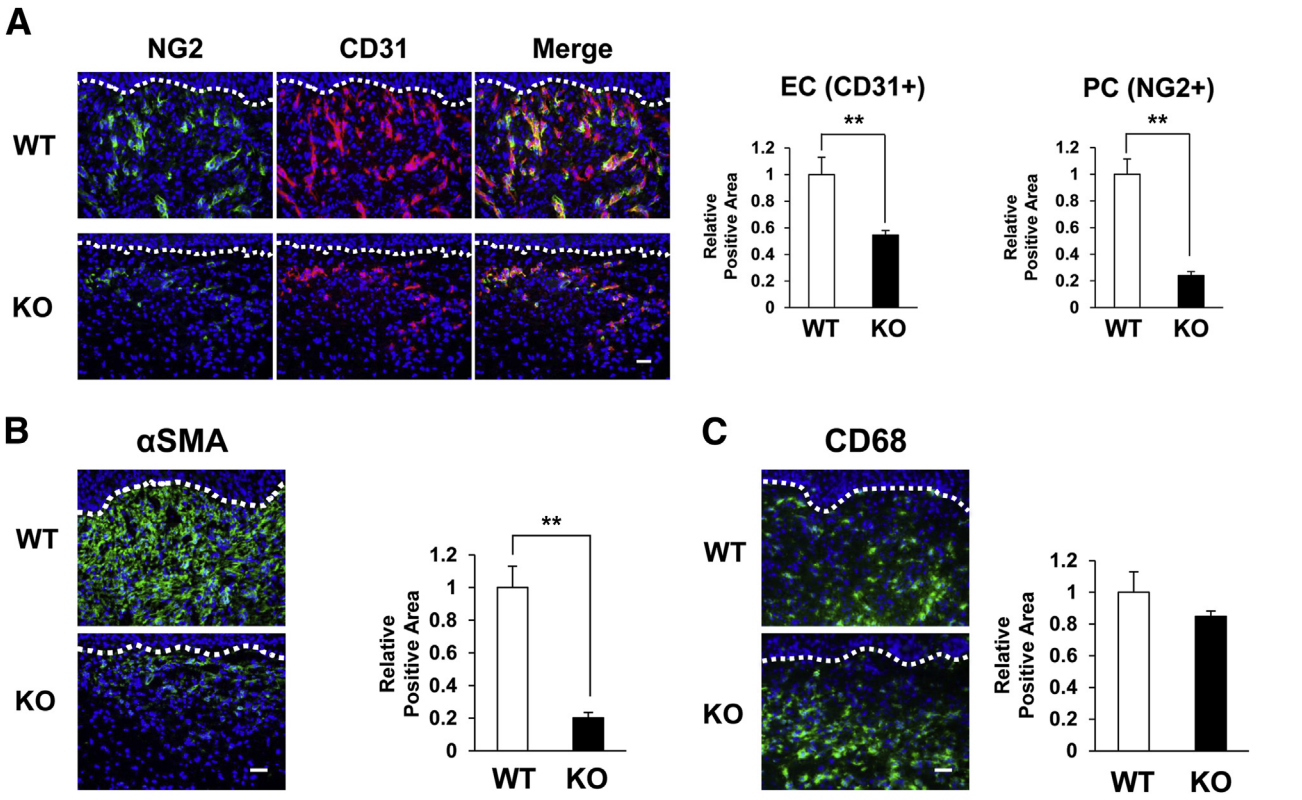

Figure 4 Blood vessels and myofibroblasts in wound areas are reduced in MFG-E8 KO mice. **A:** Distribution of ECs ($CD31^+$) and pericytes ($NG2^+$) in the granulation tissue in the wound in MFG-E8 WT and KO C57BL/6 mice at 7 days after wounding. **B:** Distribution of αSMA^+ pericytes or myofibroblasts in the dermis of wounds in MFG-E8 WT/KO C57BL/6 mice at 7 days after wounding. **C:** Distribution of $CD68^+$ macrophages in the dermis of wounds in MFG-E8 WT/KO C57BL/6 mice at 7 days after wounding. **A**–**C:** Quantification of the $CD31^+$, $NG2^+$, αSMA^+, and $CD68^+$ areas in eight random microscopic fields was performed using ImageJ software. Positive areas in WT mice were assigned values of 1. The **dotted lines** indicate the border between the epidermis and the dermis. Data are expressed as means ± SEM. $n = 3$ mice per genotype. $^{**}P < 0.01$, Student's *t*-test. Scale bar = 20 μm.

regulates cutaneous wound healing during the tissue-formation phase, which is characterized by the formation of granulation tissue and new blood vessels and occurs from 2 to 10 days after wounding.

Reduced Frequencies of Blood Vessels and Myofibroblasts in Wound Areas in MFG-E8 KO Mice

Because MFG-E8 accumulated around blood vessels in granulation tissue, we examined the influence of MFG-E8 on vascularity in wound areas. At 7 days after wounding, the number of $CD31^+$ ECs and $NG2^+$ pericytes in wound areas in MFG-E8 KO mice was decreased by 50% to 70%, compared with WT mice (Figure 4A). These results suggest that MFG-E8 enhances angiogenesis in granulation tissue during the tissue-formation phase of skin wound healing.

Fibroblasts are attracted from the edges of wounds or from bone marrow during the tissue-formation phase of wound healing.[31] Activation of fibroblasts causes differentiation into myofibroblasts that express αSMA.[32,33] Furthermore, it has also been reported that pericytes in skin and kidney can differentiate into myofibroblasts.[34,35] Myofibroblasts facilitate wound healing by remodeling extracellular matrix, secreting growth factors, and causing wound contracture. The amount of αSMA^+ pericytes or myofibroblasts in the granulation tissue in MFG-E8 KO mice was reduced by approximately 80%, compared with WT mice (Figure 4B), suggesting that MFG-E8 might be involved in the differentiation of pericytes into myofibroblasts and/or in the migration of myofibroblast precursors.

During the tissue-formation phase of wound healing, recruited macrophages secrete growth factors (including VEGF and PDGF) and induce angiogenesis.[1,2] We therefore quantified macrophages in granulation tissue in MFG-E8 WT and KO mice. Numbers of $CD68^+$ macrophages in granulation tissue did not differ between MFG-E8 WT and KO mice (Figure 4C), suggesting that the delay of wound healing in MFG-E8 KO mice cannot be attributed to reduced macrophage infiltration.

Inhibition of the Formation of Capillary-Like Structures Composed of Pericyte-Like Cells and Endothelial Cells by MFG-E8 siRNAs

Seeking a direct link of MFG-E8 to angiogenesis, we examined the effects of MFG-E8 depletion in a capillary-like structure formation assay *in vitro* using HUVECs and murine C3H 10T1/2 cells as surrogates for pericytes and

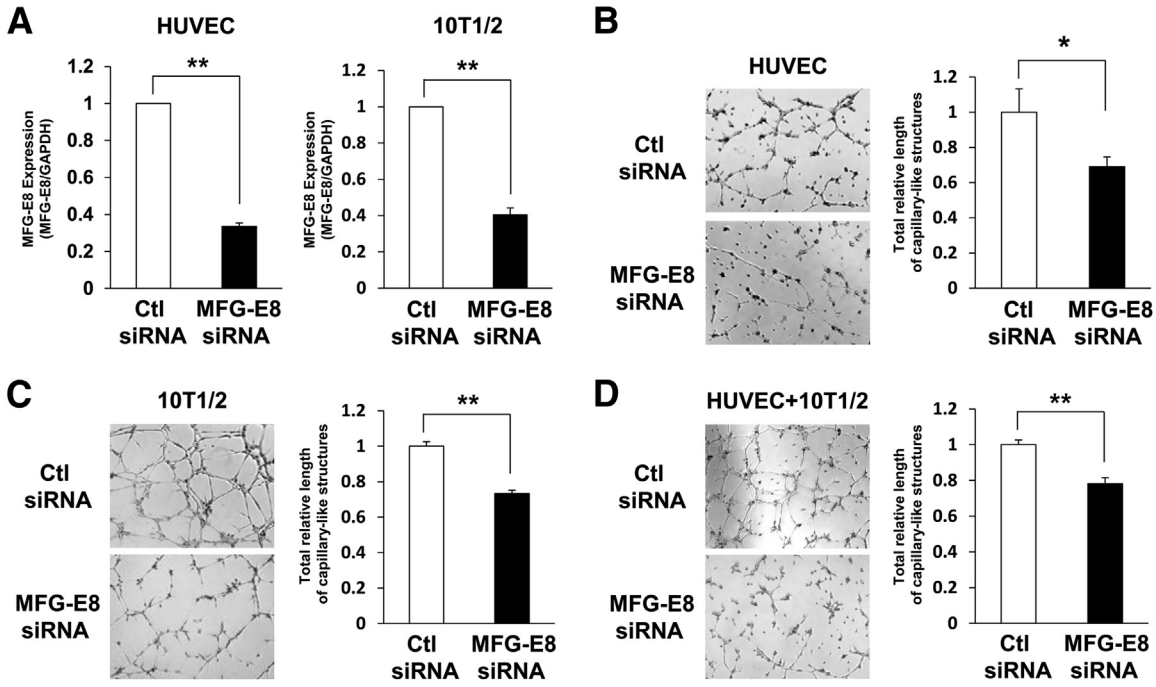

Figure 5 MFG-E8 siRNAs inhibit formation of capillary-like structures of pericyte-like cells and endothelial cells. **A:** Inhibition of MFG-E8 mRNA expression after transfection of ECs (HUVEC) or pericyte-like cells (10T1/2) with siRNAs, determined using RT-qPCR. **B**–**D:** Inhibition of the formation of capillary-like structures by ECs (HUVEC) (**B**), pericyte-like cells (10T1/2) (**C**), and both ECs and pericyte-like cells (**D**) using MFG-E8 siRNAs is shown in images. Quantification of total relative length of capillary-like structures of ECs and/or pericyte-like cells in six random microscopic fields in three independent experiments was performed using ImageJ software. Data are expressed as means ± SEM, normalized to networks formed by control siRNA-treated cells, from three independent experiments. $*P < 0.05$, $**P < 0.01$ versus control, Student's *t*-test. Original magnification, ×40. Ctl, control.

pericyte precursors. HUVECs and pericyte-like cells (10T1/2) were depleted of MFG-E8 with siRNA and cocultured on Matrigel. In these experiments, we achieved a marked reduction of MFG-E8 mRNA and protein levels in both HUVECs and 10T1/2 cells (Figure 5A and Supplemental Figure S2). Depletion of MFG-E8 in ECs (HUVECs) reduced formation of capillary-like structures (Figure 5B). Depletion of MFG-E8 in pericyte-like cells (10T1/2) also reduced formation of capillary-like structures (Figure 5C). Furthermore, depletion of MFG-E8 in both ECs and pericyte-like cells reduced formation of capillary-like structures by approximately 20% (Figure 5D). These results suggest that MFG-E8 derived from ECs, pericytes, or both cell types might regulate angiogenesis.

Accumulation and Distribution of MFG-E8 in Close Proximity to Pericytes in Human Granulation Tissue

Fibrous granulation tissue is a characteristic of nonhealing wounds. Fibrous granulation tissue from intractable ulcers contained smaller numbers of blood vessels, compared with better vascularized normal granulation tissue (Figure 6, A and B). We examined the localization and amount of MFG-E8 in human normal and fibrous granulation tissue. In both normal and fibrous granulation tissue, MFG-E8 localized around $CD31^+$ ECs and colocalized with αSMA^+ pericytes (Figure 6C), as we had demonstrated in granulation tissue in murine skin wounds (Figure 2, E and F). Lesser amounts of MFG-E8 were present in fibrous granulation tissue with scant vessels, compared with normal granulation tissue, which contained many blood vessels (Figure 6D). These results suggest that MFG-E8 might regulate angiogenesis in human as well as in mouse granulation tissue.

Discussion

Using immunofluorescence, we determined that MFG-E8 accumulated around $CD31^+$ ECs and colocalized with αSMA^+ or $PDGFR\beta^+$ pericytes in human and murine dermis. These results are consistent with our previous findings, that MFG-E8 colocalized with $PDGFR\beta^+$ pericytes in B16 melanoma tumors.[23] Because MFG-E8 is a secreted protein, this result does not prove that MFG-E8 originates in dermal pericytes. However, we had previously demonstrated (using fluorescence-activated cell sorting and qPCR) that pericytes in melanoma tissues produce MFG-E8,[23] which suggests that pericytes are likely to be a major source of MFG-E8 in the dermis in normal murine and human skin.

In the process of wound healing, tissue formation occurs from 2 to 10 days after wounding and is characterized by epithelialization, the formation of granulation tissue and new blood vessels, and the migration of macrophages and fibroblasts. MFG-E8 protein and mRNA levels were increased in granulation tissue in wound areas from 4 to 14

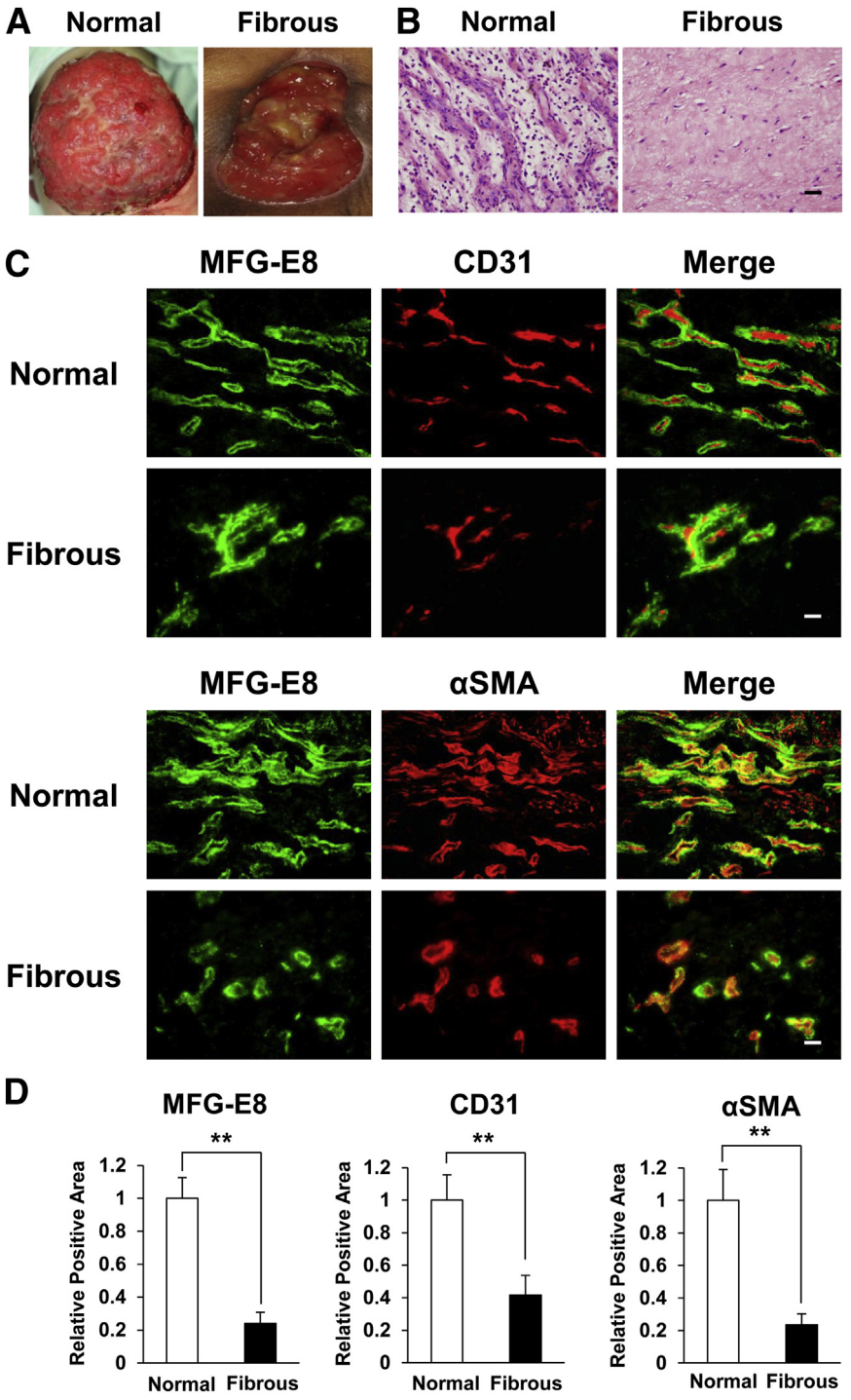

Figure 6 Accumulation and distribution of MFG-E8 in close proximity to pericytes in human granulation tissue. **A:** Clinical appearance of normal granulation tissue in decubitus ulcer and fibrous granulation tissue in intractable decubitus ulcer. **B:** Histological appearance of normal and fibrous human granulation tissue. H&E stain. **C:** Localization of MFG-E8 in relationship to endothelial cells ($CD31^+$) or pericytes (αSMA^+) in human granulation tissue. **D:** Quantification of the extent of MFG-E8 expression, $CD31^+$ ECs, and αSMA^+ pericytes in normal and fibrous granulation tissue in eight random microscopic fields in three independent experiments was performed using ImageJ software. Positive area in normal granulation tissue was assigned a value of 1. Data are expressed as means ± SEM. $n = 3$. $^{**}P < 0.01$, Student's *t*-test. Scale bar = 20 μm.

days after wounding. In addition, in both BALB/c and C57BL/6 mice, wound healing was significantly delayed in MFG-E8 KO mice. Addition of rMFG-E8 into wounds reversed the inhibition of wound healing caused by MFG-E8 knockdown. These results suggest that MFG-E8 might promote wound healing during the tissue-formation phase. Wound healing is delayed in MFG-E8 KO mice of both C57BL and BALB/c backgrounds during the tissue-formation phase. However, wounds in KO mice eventually heal completely, and by the same time points as in the WT mice. The explanations for this observation are unknown. We measured wound size every other day, not every day, and so we might not detect small differences (<2 days) in wound closure time between WT and KO mice.

MFG-E8 was diffusely distributed in granulation tissue, with accumulations around $CD31^+$ ECs and more extensive association with αSMA^+ pericytes or myofibroblasts. $CD31^+$ EC numbers were reduced in granulation tissue in MFG-E8

KO mice, and $NG2^+$ pericyte numbers in MFG-E8 KO mice were also reduced. These results are consistent with our previous findings of reduced numbers of $PDGFR\beta^+$ pericytes and $CD31^+$ ECs in melanoma tumors from MFG-E8 KO mice.[23] The present results suggest that MFG-E8 might promote wound healing during the tissue-formation phase by enhancing angiogenesis in granulation tissue.

Consistent with this hypothesis, depletion of MFG-E8 in ECs and pericyte-like cells using siRNA attenuated the formation of capillary-like structures *in vitro*. We had previously determined that MFG-E8 enhances PDGF-stimulated migration of pericytes-like 10T1/2 cells via enhancement of PDGF:PDGFRβ signaling-mediated integrin-growth factor receptor crosstalk,[24] and others have demonstrated that ECs require MFG-E8 for VEGF-induced proliferation and survival.[20] We speculate, therefore, that MFG-E8 is produced primarily by pericytes or myofibroblasts and acts on pericytes and ECs by potentiating the stimulatory effects of PDGF and VEGF, respectively, thus leading to enhanced angiogenesis.

Myofibroblasts play important roles in wound healing through matrix remodeling, growth factor secretion, and wound contraction.[36] Recently, both fibroblasts and pericytes have been reported to be myofibroblast precursors.[24,35] In addition, it has been reported that pericytes and fibroblasts are derived from mesenchymal stem cells, and that they can transdifferentiate into each other.[4,37] In the present study, MFG-E8 was associated with αSMA^+ pericytes or myofibroblasts in granulation tissue, and the number of αSMA^+ pericytes or myofibroblasts in granulation tissue in MFG-E8 KO mice was significantly inhibited, compared with WT mice. Perhaps MFG-E8 is involved in the differentiation of precursors into myofibroblast or in the migration of myofibroblasts precursors.

We had previously demonstrated that depletion of MFG-E8 in pericyte-like cells (10T1/2) did not alter TGF-β-induced differentiation into myofibroblasts.[23] In those analyses, however, PDGF-dependent pericyte-like cell (10T1/2) migration was inhibited by the depletion of MFG-E8 using siRNA.[23] Furthermore, it has been reported that blocking PDGFRβ signaling inhibited proliferation and migration of fibroblasts and pericytes, but did not prevent the differentiation into myofibroblasts *in vitro*.[3] Taken together, these results suggest that MFG-E8 might regulate migration of myofibroblast precursors, including fibroblasts and pericytes into wounds, but not differentiation into myofibroblasts.

Myofibroblasts are responsible for wound contracture. In the present study, the numbers of myofibroblasts in wound areas in MFG-E8 KO mice were reduced, but wound closure time did not differ markedly between MFG-E8 WT and KO mice. Recently, it has been reported that tissue tension generated by myofibroblasts pulled vessels into granulation tissue from pre-existing vascular beds as vascular loops with functional circulation, suggesting that contractile forces of myofibroblasts might contribute to angiogenesis.[38] This in turn suggests that reductions in myofibroblasts in wound areas in MFG-E8 KO mice might be associated with decreased vascularity, highlighting another mechanism by which MFG-E8 may regulate angiogenesis.

Our present findings implicate MFG-E8 in skin wound healing. At steady state, MFG-E8 appears to be mainly produced by ECs and pericytes, and MFG-E8 localizes around blood vessels. In response to injury or wounding, MFG-E8 accumulation and expression is enhanced in granulation tissue and around blood vessels. MFG-E8 may enhance angiogenesis in granulation tissue by acting directly on ECs or pericytes. MFG-E8 might also enhance migration of pericytes or fibroblasts into wound areas, leading to increases in myofibroblasts. In aggregate, these activities of MFG-E8 promote skin wound healing. MFG-E8 may also regulate pericyte or fibroblast migration via enhancement of PDGFRβ signaling. Finally, we demonstrated that MFG-E8 localized around $CD31^+$ ECs and associated with αSMA^+ pericytes in human granulation tissue, and that MFG-E8 expression in fibrous granulation tissue with scant blood vessels was less than that in normal granulation tissue with abundant vessels, suggesting that MFG-E8 might regulate angiogenesis in human granulation tissue. Additional studies are needed to elucidate the roles of MFG-E8 in the regulation of wound healing in humans, including examination of angiogenesis, contraction, and differentiation of fibroblasts. It may be that abnormalities in MFG-E8 production or function contribute to the intractable wound healing that causes considerable morbidity in patients with diabetic or decubitus ulcers. MFG-E8 may have utility as a therapeutic in these difficult cases.

Acknowledgments

We thank Drs. Yayoi Nagai and Etsuko Okada (Gunma University Graduate School of Medicine, Maebashi, Japan) for help with preparing human skin samples.

Supplemental Data

Supplemental material for this article can be found at *http://dx.doi.org/10.1016/j.ajpath.2014.03.017*.

References

1. Gurtner GC, Werner S, Barrandon Y, Longaker MT: Wound repair and regeneration. Nature 2008, 453:314–321
2. Singer AJ, Clark RA: Cutaneous wound healing. N Engl J Med 1999, 341:738–746
3. Rajkumar VS, Shiwen X, Bostrom M, Leoni P, Muddle J, Ivarsson M, Gerdin B, Denton CP, Bou-Gharios G, Black CM, Abraham DJ: Platelet-derived growth factor-beta receptor activation is essential for fibroblast and pericyte recruitment during cutaneous wound healing. Am J Pathol 2006, 169:2254–2265
4. Eming SA, Brachvogel B, Odorisio T, Koch M: Regulation of angiogenesis: wound healing as a model. Prog Histochem Cytochem 2007, 42:115–170
5. Stubbs JD, Lekutis C, Singer KL, Bui A, Yuzuki D, Srinivasan U, Parry G: cDNA cloning of a mouse mammary epithelial cell surface

protein reveals the existence of epidermal growth factor-like domains linked to factor VIII-like sequences. Proc Natl Acad Sci USA 1990, 87:8417–8421
6. Ogura K, Nara K, Watanabe Y, Kohno K, Tai T, Sanai Y: Cloning and expression of cDNA for O-acetylation of GD3 ganglioside. Biochem Biophys Res Commun 1993, 225:932–938
7. Taylor MR, Couto JR, Scallan CD, Ceriani RL, Peterson JA: Lactadherin (formerly BA46), a membrane-associated glycoprotein expressed in human milk and breast carcinomas, promotes Arg-Gly-Asp (RGD)-dependent cell adhesion. DNA Cell Biol 1997, 16:861–869
8. Andersen MH, Berglund L, Rasmussen JT, Petersen TE: Bovine PAS-6/7 binds alpha v beta 5 integrins and anionic phospholipids through two domains. Biochemistry 1997, 36:5441–5446
9. Raymond A, Ensslin MA, Shur BD: SED1/MFG-E8: a bi-motif protein that orchestrates diverse cellular interactions. J Cell Biochem 2009, 106:957–966
10. Hanayama R, Tanaka M, Miwa K, Shinohara A, Iwamatsu A, Nagata S: Identification of a factor that links apoptotic cells to phagocytes. Nature 2002, 417:182–187
11. Ensslin MA, Shur BD: The EGF repeat and discoidin domain protein, SED1/MFG-E8, is required for mammary gland branching morphogenesis. Proc Natl Acad Sci USA 2007, 104:2715–2720
12. Shi J, Heegaard CW, Rasmussen JT, Gilbert GE: Lactadherin binds selectively to membranes containing phosphatidyl-L-serine and increased curvature. Biochim Biophys Acta 2004, 1667:82–90
13. Shao C, Novakovic VA, Head JF, Seaton BA, Gilbert GE: Crystal structure of lactadherin C2 domain at 1.7A resolution with mutational and computational analyses of its membrane-binding motif. J Biol Chem 2008, 283:7230–7241
14. Asano K, Miwa M, Miwa K, Hanayama R, Nagase H, Nagata S, Tanaka M: Masking of phosphatidylserine inhibits apoptotic cell engulfment and induces autoantibody production in mice. J Exp Med 2004, 200:459–467
15. Hanayama R, Tanaka M, Miyasaka K, Aozasa K, Koike M, Uchiyama Y, Nagata S: Autoimmune disease and impaired uptake of apoptotic cells in MFG-E8-deficient mice. Science 2004, 304:1147–1150
16. Hanayama R, Nagata S: Impaired involution of mammary glands in the absence of milk fat globule EGF factor 8. Proc Natl Acad Sci USA 2005, 102:16886–16891
17. Miksa M, Wu R, Dong W, Komura H, Amin D, Ji Y, Wang Z, Wang H, Ravikumar TS, Tracey KJ, Wang P: Immature dendritic cell-derived exosomes rescue septic animals via milk fat globule epidermal growth factor-factor VIII. J Immunol 2009, 183:5983–5990
18. Ait-Oufella H, Kinugawa K, Zoll J, Simon T, Boddaert J, Heeneman S, Blanc-Brude O, Barateau V, Potteaux S, Merval R, Esposito B, Teissier E, Daemen MJ, Lesèche G, Boulanger C, Tedgui A, Mallat Z: Lactadherin deficiency leads to apoptotic cell accumulation and accelerated atherosclerosis in mice. Circulation 2007, 115:2168–2177
19. Boddaert J, Kinugawa K, Lambert JC, Boukhtouche F, Zoll J, Merval R, Blanc-Brude O, Mann D, Berr C, Vilar J, Garabedian B, Journiac N, Charue D, Silvestre JS, Duyckaerts C, Amouyel P, Mariani J, Tedgui A, Mallat Z: Evidence of a role for lactadherin in Alzheimer's disease. Am J Pathol 2007, 170:921–929
20. Silvestre JS, Théry C, Hamard G, Boddaert J, Aguilar B, Delcayre A, Houbron C, Tamarat R, Blanc-Brude O, Heeneman S, Clergue M, Duriez M, Merval R, Lévy B, Tedgui A, Amigorena S, Mallat Z: Lactoadherin promotes VEGF-dependent neovascularization. Nat Med 2005, 11:499–506
21. Ensslin MA, Shur BD: Identification of mouse sperm SED1, a bimotif EGF repeat and discoidin-domain protein involved in sperm-egg binding. Cell 2003, 114:405–417
22. Atabai K, Jame S, Azhar N, Kuo A, Lam M, McKleroy W, Dehart G, Rahman S, Xia DD, Melton AC, Wolters P, Emson CL, Turner SM, Werb Z, Sheppard D: Mfge8 diminishes the severity of tissue fibrosis in mice by binding and targeting collagen for uptake by macrophages. J Clin Invest 2009, 119:3713–3722
23. Motegi S, Leitner WW, Lu M, Tada Y, Sárdy M, Wu C, Chavakis T, Udey MC: Pericyte-derived MFG-E8 regulates pathologic angiogenesis. Arterioscler Thromb Vasc Biol 2011, 31:2024–2034
24. Motegi S, Garfield S, Feng X, Sárdy M, Udey MC: Potentiation of platelet-derived growth factor receptor-β signaling mediated by integrin-associated MFG-E8. Arterioscler Thromb Vasc Biol 2011, 31: 2653–2664
25. Bu HF, Zuo XL, Wang X, Ensslin MA, Koti V, Hsueh W, Raymond AS, Shur BD, Tan XD: Milk fat globule-EGF factor 8/lactadherin plays a crucial role in maintenance and repair of murine intestinal epithelium. J Clin Invest 2007, 117:3673–3683
26. Neutzner M, Lopez T, Feng X, Bergmann-Leitner ES, Leitner WW, Udey MC: MFG-E8/lactadherin promotes tumor growth in an angiogenesis-dependent transgenic mouse model of multistage carcinogenesis. Cancer Res 2007, 67:6777–6785
27. Lin Q, Fang D, Fang J, Ren X, Yang X, Wen F, Su SB: Impaired wound healing with defective expression of chemokines and recruitment of myeloid cells in TLR3-deficient mice. J Immunol 2011, 186: 3710–3717
28. Zheng Y, Watanabe M, Kuraishi T, Hattori S, Kai C, Shibuya M: Chimeric VEGF-ENZ7/PlGF specifically binding to VEGFR-2 accelerates skin wound healing via enhancement of neovascularization. Arterioscler Thromb Vasc Biol 2007, 27:503–511
29. Darland DC, D'Amore PA: TGF beta is required for the formation of capillary-like structures in three-dimensional cocultures of 10T1/2 and endothelial cells. Angiogenesis 2001, 4:11–20
30. Bryan BA, D'Amore PA: Pericyte isolation and use in endothelial/pericyte coculture models. Methods Enzymol 2008, 443:315–331
31. Opalenik SR, Davidson JM: Fibroblast differentiation of bone marrow-derived cells during wound repair. FASEB J 2005, 19:1561–1563
32. Darby I, Skalli O, Gabbiani G: Alpha-smooth muscle actin is transiently expressed by myofibroblasts during experimental wound healing. Lab Invest 1990, 63:21–29
33. Li B, Wang JH: Fibroblasts and myofibroblasts in wound healing: force generation and measurement. J Tissue Viability 2011, 20:108–120
34. Sponheim J, Pollheimer J, Olsen T, Balogh J, Hammarström C, Loos T, Kasprzycka M, Sørensen DR, Nilsen HR, Küchler AM, Vatn MH, Haraldsen G: Inflammatory bowel disease-associated interleukin-33 is preferentially expressed in ulceration-associated myofibroblasts. Am J Pathol 2010, 177:2804–2815
35. Chen YT, Chang FC, Wu CF, Chou YH, Hsu HL, Chiang WC, Shen J, Chen YM, Wu KD, Tsai TJ, Duffield JS, Lin SL: Platelet-derived growth factor receptor signaling activates pericyte-myofibroblast transition in obstructive and post-ischemic kidney fibrosis. Kidney Int 2011, 80:1170–1181
36. Hinz B, Phan SH, Thannickal VJ, Galli A, Bochaton-Piallat ML, Gabbiani G: The myofibroblast: one function, multiple origins. Am J Pathol 2007, 170:1807–1816
37. Rønnov-Jessen L, Petersen OW, Koteliansky VE, Bissell MJ: The origin of the myofibroblasts in breast cancer. Recapitulation of tumor environment in culture unravels diversity and implicates converted fibroblasts and recruited smooth muscle cells. J Clin Invest 1995, 95: 859–873
38. Kilarski WW, Samolov B, Petersson L, Kvanta A, Gerwins P: Biomechanical regulation of blood vessel growth during tissue vascularization. Nat Med 2009, 15:657–664